ELSEVIER

PII: S0032-3861(97)10241-5

Polymer Vol. 39 No. 15, pp. 3523–3528, 1998

0032-3861/98/$19.00+0.00

Structural features of the mesomorphic form of syndiotactic poly(*p*-methylstyrene)

Odda Ruiz de Ballesteros, Finizia Auriemma, Claudio De Rosa*, Giovanni Floridi and Vittorio Petraccone

Università di Napoli 'Federico II', Dipartimento di Chimica, Via Mezzocannone, 4 80134 Napoli, Italy

(Accepted 13 October 1997)

A possible structural model for the mesomorphic form of syndiotactic poly(*p*-methylstyrene) is discussed. The structural analysis is performed through the comparison between the experimental X-ray diffraction intensities and the calculated intensities for model structures constituted by ordered and disordered aggregates of chains. This analysis provides support for the hypothesis that the mesomorphic form of sPPMS may be described in terms of small aggregates of *trans*-planar chains having a packing mode very close to that one of form III, in which disorder in the relative arrangement of neighbouring chains is present to some extent. © 1998 Elsevier Science Ltd. All rights reserved.

(Keywords: syndiotactic poly(*p*-methystyrene); mesomorphic form; structure)

INTRODUCTION

It is well established that homogenous catalytic systems based on titanium or zirconium compounds and methylaluminoxane are able to produce highly syndiotactic polystyrene (sPS)[1,2]. Using these catalytic systems it is also possible to obtain substituted polystyrenes with a high degree of syndiotacticity, as in the case of poly(*p*-methylstyrene) (sPPMS)[3–8].

The very complex polymorphic behaviour[9–11] and the crystal structures of various modifications of sPS[12–18] have been reported.

Structural studies[19–22] have also revealed a complex polymorphic behaviour for sPPMS. In fact, four different crystalline forms (I, II, III and V) and a mesomorphic form (IV), as well as several clathrate structures, have been found. *FT*i.r. and solid-state ^{13}C-n.m.r. studies on the different forms of sPPMS, combined with X-ray diffraction data[20–22], have shown that the chain conformations involved in the various modifications are the same as found for sPS: *trans*-planar and s(2/1)2 helical. In particular, forms I and II and all the clathrate structures of sPPMS present chains in the s(2/1)2 helical conformation, with a chain periodicity $c = 7.8$ Å[22]; forms III, IV and V, instead, present chains in *trans*-planar conformation, with a chain periodicity $c = 5.1$ Å[22,23].

The crystal structure of form III of sPPMS is the only one solved up to now. It is composed of *trans*-planar chains packed in an orthorhombic unit cell with axes $a = 13.36$ Å, $b = 23.21$ Å and $c = 5.12$ Å. The proposed space group is *Pnam*[23]. We recall that oriented samples of form III can be easily obtained by annealing fibres of sPPMS in the mesomorphic modification, at a temperature of nearly 210°C[23].

In the present paper an analysis of the structure of the mesomorphic form IV of sPPMS, through comparison between the experimental intensities, collected by an automatic diffractometer, and the results of Fourier transform calculations on model structures are presented. The models are constituted by aggregates of *trans*-planar chains, in which various kinds of disorder in the relative arrangement of the chains, are introduced.

EXPERIMENTAL SECTION

sPPMS was synthesized as described in Ref. 8. The syndiotacticity of the polymer was evaluated by ^{13}C-n.m.r.[8]; the fraction of the pentads *rrrr* is higher than 95%.

Oriented samples of sPPMS in the mesomorphic form IV can be obtained by drawing films of both crystalline forms I and II, as well as of any clathrate structure or of samples in the amorphous phase. In the present case crystalline samples of form I were stretched at 135°C, using a Polymer Lab miniature material tester, at a strain rate of 1 mm/min, with an initial gauge length of 8 mm up to a strain ratio of nearly 3:1. The measured density (obtained by flotation) results equal to 1.02 g/cm^3, as in the amorphous phase.

The X-ray diffraction patterns, with Ni-filtered Cu–Kα radiation, were obtained by using a Nonius automatic CAD4 diffractometer, always maintaining an equatorial geometry. The measurements have been performed along the reciprocal cylindrical co-ordinate ξ in the range $0 < \xi < 0.6$ Å^{-1}, at intervals of 0.006 Å^{-1}, for $\zeta = l/c$ ($l = 0, 1, 2, 3, 4$ and $c = 5.08$ Å, being the chain periodicity) and along the reciprocal co-ordinate ζ in the range $0 < \xi < 0.8$ Å^{-1}, at the same intervals, for $\zeta = 0$.

The calculated intensities to be compared with the experimental ones have been corrected for the Lorentz and polarization factor (Lp) that is, according to the diffraction geometry, $Lp = (1 + \cos^2 2\theta)/\sin 2\theta$.

X-RAY DIFFRACTION ANALYSIS

The X-ray fibre diffraction photographic pattern of the mesomorphic form of sPPMS has been reported elsewhere[22]. The X-ray diffraction intensities of a fibre of

* To whom correspondence should be addressed

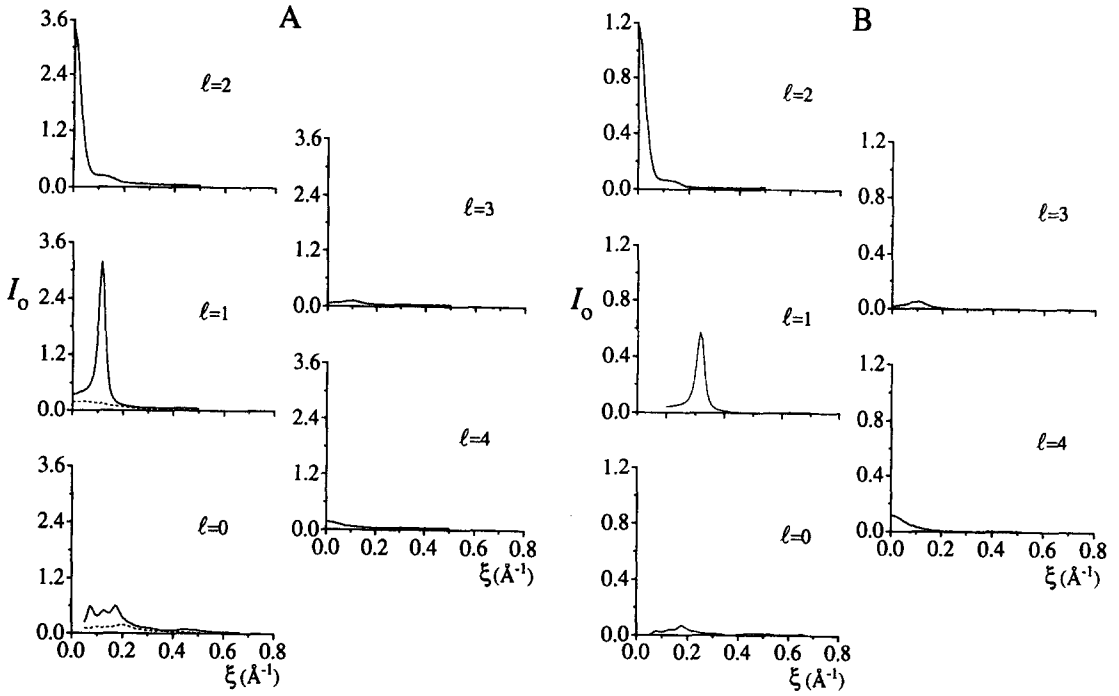

Figure 1 Experimental X-ray diffraction intensity of a fibre of sPPMS in the mesomorphic form *versus* the cylindrical co-ordinate ξ for the indicated layer lines (corresponding to a periodicity of $c = 5.08$ Å) before (A) and after the subtraction of the background and the amorphous contribution and after correction for the *Lp* factor (B). The dashed lines indicate the amorphous contribution

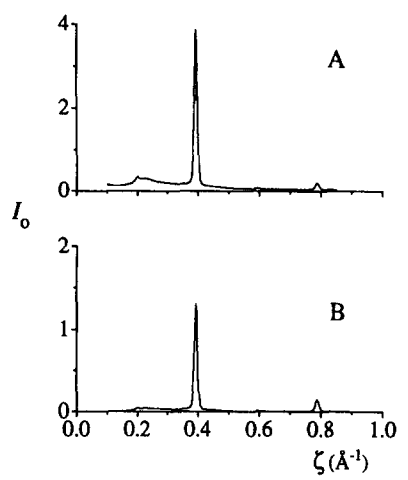

Figure 2 Experimental X-ray diffraction intensity of a fibre of sPPMS in the mesomorphic form *versus* the cylindrical co-ordinate ζ on the meridian ($\xi = 0$) before (A) and after the subtraction of the background and correction for the *Lp* factor (B)

sPPMS in the mesomorphic form, collected along the layer lines with $\ell = 0, 1, 2, 3, 4$ and along the meridian ($\xi = 0$), are reported in *Figures 1A* and *2A*, respectively. The same, after the subtraction of the background and of the amorphous contribution and after correction for the *Lp* factor, are reported in *Figures 1B* and *2B*, respectively. The dashed lines in *Figure 1A* indicate the amorphous contribution. It is drawn, suitably scaling along the ξ-axis the measured diffraction intensity along the layer line at $\zeta = 0.098$ Å^{-1} ($= 0.5/c$, where the mesomorphic form does not contribute to the diffraction).

Some important features of the experimental patterns of *Figures 1B* and *2B* are listed below:

(1) the equator ($\ell = 0$) is characterized by three broad peaks, centred at $\xi \approx 0.07$ Å, $\xi \approx 0.12$ Å^{-1} and $\xi \approx 0.17$ Å^{-1};

(2) on the first layer line ($\ell = 1$) only a strong diffraction peak, with half-height width (W(1)) of about 0.35 Å^{-1}, at $\xi = 0.112$ Å^{-1} is present. The ratio between the integrated intensity of this peak, in the range $0 < \xi < 0.2$ Å^{-1} and the integrated intensity along the equatorial profile, in the range $0.06 < \xi < 0.25$ Å^{-1}, ($I(1)/I(0)$) is nearly 4.4;

(3) on the third layer line ($\ell = 3$) a very diffuse halo centred at $\xi = 0.10$ Å^{-1} is present;

(4) both second ($\ell = 2$) and fourth ($\ell = 4$) layer lines present single peaks with maxima at $\xi = 0$ (meridional reflections) corresponding to a chain periodicity of 5.08 Å. They are broad along ξ and sharp along ζ (compare *Figures 1B* and *2B*). The half-height width of the peak on the second layer line along ξ (W(2)) is nearly 0.05 Å^{-1}.

In summary, the absence of sharp reflections on the equator and the presence of broad peaks on nonequatorial layer lines indicates that a long-range order is possibly maintained only along the chain axis (the backbone conformation remaining *trans*-planar). A substantial intermolecular disorder in the lateral packing between neighbouring chains is expected.

MODEL STRUCTURES FOR TRIAL CALCULATIONS

It is worth noting that the X-ray fibre diffraction pattern of sPPMS in the mesomorphic form presents some analogies with the X-ray fibre diffraction profile of sPS in the mesomorphic form[14]. In fact, both present broad halos on the equator and on the third layer line, a very strong reflection on the first layer line, and two meridional reflections (narrow along ζ, broad along ξ) on the second and fourth layer lines. The mesomorphic forms of sPS has been interpreted as composed of small, imperfect crystals of the trigonal crystallined form[14], in which the chains, in *trans*-planar conformation, are organized in triplets[12,24]. An

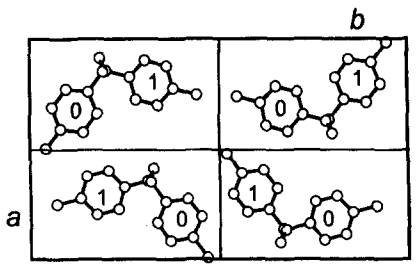

Figure 3 *ab* projection of the limit-ordered orthorhombic model structure of form III of sPPMS. The numbers indicate the relative heights of the centres of the phenyl rings in *c*/2 units

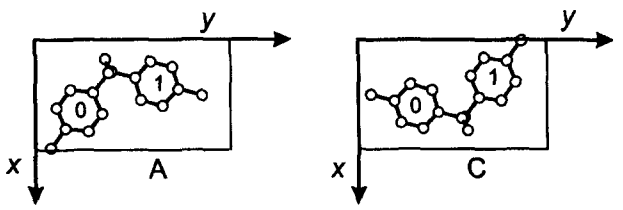

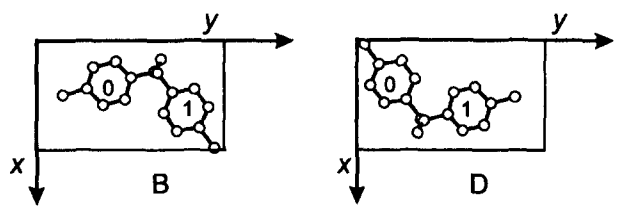

Figure 4 The chains that are the bricks of the orthorhombic structural models of form III of sPPMS, as well as of the proposed structural model of the mesomorphic form IV of sPPMS, named as A, B, C and D (see text) in the *ab* projection. The numbers indicate the relative heights of the centres of the phenyl rings in *c*/2 units

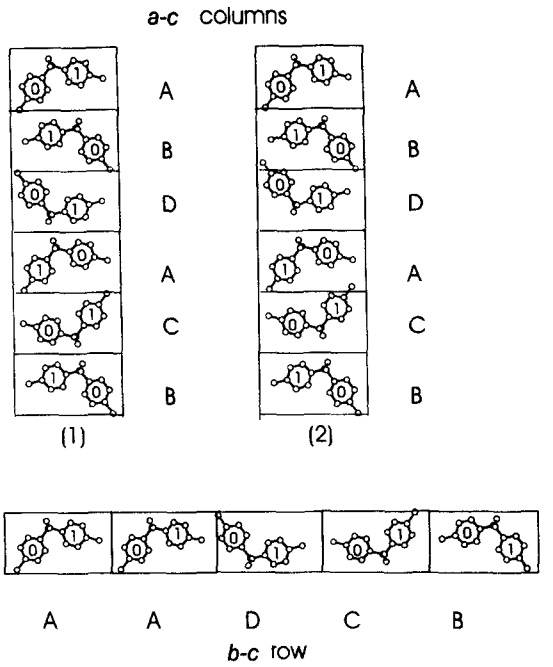

Figure 5 *a–c* columns and a *b–c* row of sPPMS chains, in which the A, B, C and D chains follow each other according to a disordered pattern. In column 2 the chains D and C in the couples of consecutive chains BD and AC come close to the chains B and A with respect to column 1, without changing the average density. This also improves the bad contact distances between the backbone atoms of consecutive DA and CB chains present in column 1. The numbers enclosed in the phenyl rings indicate their relative height along *z* in *c*/2 units

analogous, ideal, limit-ordered structure could, at least in principle, be drawn for sPPMS in the mesomorphic form, compatibly with the experimental density value and low packing energy requirements. We have proved that contrary to the α form of sPS, where the triplets are arranged observing rhombohedral shifts along *c*[12,24], an analogous rhombohedral arrangement of the triplets of chains of sPPMS is not energetically feasible, because it produces too short distances between the methyl groups belonging to adjacent triplets. Instead, we have verified (by simple packing energy calculations not reported here) that low values of the packing energy are obtained only when the heights of the phenyl rings of the triplets are equal to 0 and *c*/2, as for the model structure proposed by Greis *et al.* for the α form of sPS[25]. Anyway, Fourier transform calculations on such models gave a bad agreement with the experimental X-ray diffraction profiles, because the ratio between the integrated intensities of the peak on the first layer line and those on the equator was too low (not higher than 1.5), with respect to the experimental value, whatever the dimension of the aggregates. For this reason, model structures with sPPMS chains organized in triplets were discarded and packing models with chains faced according to the orthorhombic model structure proposed for the form III of sPPMS[23] were considered.

The orthohombic model structure of the crystalline form III of sPPMS in the space group *Pnam* (a = 13.36 Å, b = 23.21 Å, c = 5.12 Å), proposed by De Rosa *et al.*[23], is shown in *Figure 3*. It is useful to name the chains as A, B, C and D as shown in *Figure 4* according to their orientation around the chain axis and according to their position in a quarter of the unit cell of form III (compare with *Figure 3*). The limit-ordered orthorombic model structure for the form III may be described in terms of *a–c* columns of chains ...ABAB... and ...CDCD... alternating along *b* or in terms of *b–c* rows of chains ...ACAC... and ...BDBD... alternating along *a* providing that a local co-ordinate system is associated to each chain such as the one shown in *Figure 4*. This local co-ordinate system is such that the translation vector relating consecutive chains in an *a–c* column is **a**/2 + **c**/2 whereas the translation vector connecting consecutive chains in a *b–c* row is **b**/2.

We have proved that different kinds of sequences of the chains A, B, C and D, both along *a* and along *b*, are allowed for at a low cost of the packing energy. *Figure 5* shows columns and a row of chains as an example, where the chains along *a* (*a–c* columns) and along *b* (*b–c* row) follow each other according to a disordered pattern. We have fixed the distances between couples of consecutive chains equal to **a**/2 + **c**/2 for the *a–c* column numbered as 1, equal to *b*/2 for the *b–c* rows, i.e. the packing density being maintained equal to the density of form III of sPPMS. It is worth noting that in some cases a shorter distance among couples of consecutive chains and/or slightly different arrangements of the chains produces locally a more efficient packing. For instance, in the case of the couples of chains BD or AC in the *a–c* column 1, the shortest distance between the carbon atoms is 4.6 Å, which is too large. At the same time, if a D chain is followed by a chain of kind A or a C chain by a chain of kind B, as in the *a–c* column 1, distances as short as

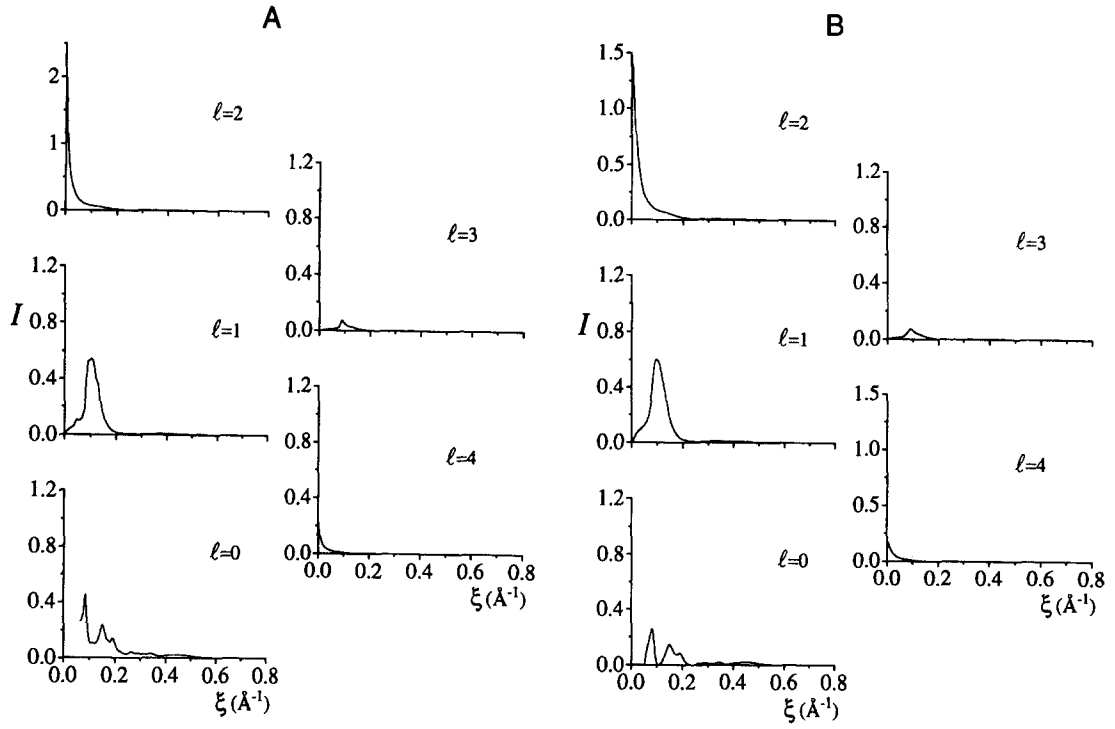

Figure 6 Calculated X-ray diffraction intensity (I) for the limit-ordered model structure of *Figure 3*: (A) $L_a = L_b = 60$ Å; (*B*) $L_a = L_b = 30$ Å. $\sigma_a \approx \sigma_b = 0.8$ Å, $\sigma_z = 1.0$ Å. $B_\xi = 12$ Å^2, $B_\zeta = 6$ Å^2

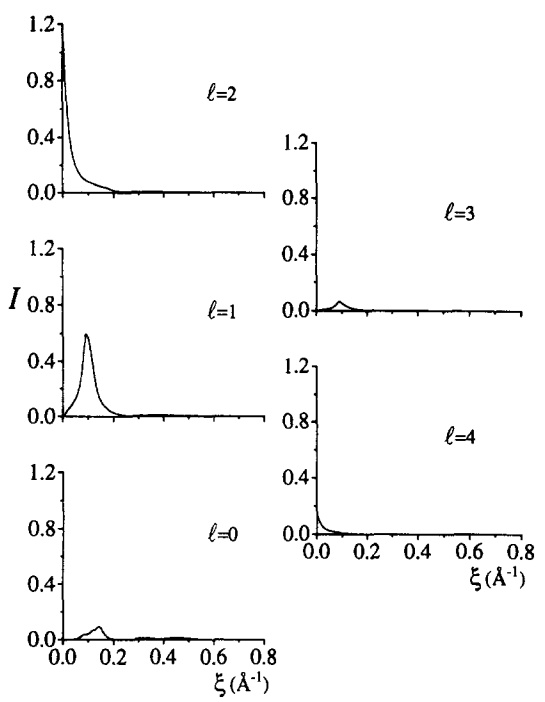

Figure 7 Calculated X-ray diffraction intensity (I) for a disordered structure model in which each site of the limit-ordered orthorhombic structure model may be occupied with equal probability by chains of kind A or D followed along a (with equal probability) by chains of kind B and C. $\sigma_a = \sigma_b = 0.8$ Å, $\sigma_z = 1.0$ Å. $B_\xi = 12$ Å^2, $B_\zeta = 6$ Å^2

2.4 Å between the backbone carbon atoms occur. Such sequences would be at best accommodated, leaving unaltered the density of form III (i.e. equal to 0.988 g/cm^3) [23], if the chain axes of the D or C chains are shifted toward the chains of kind B or A, respectively, moving along the direction a, as shown in the a–c column 2. This automatically adjusts the bad contact distances between the backbone atoms of the consecutive chains D–A and C–B in the a–c column 1 shown in the example, leading their distance equal to 3.6 Å (a–c column 2). It is worth noting that sequences of chains of kind BD and AC are particularly favourable if the chains are placed close to each other as in the a–c column 2. The occurrence of such couples of chains disturbs locally the alternation ...ABAB... or ...CDCD... of the chains along a, typical of the limit-ordered structural model of form III, and also makes possible other kinds of sequences, thus determining disorder along a. Likewise, along b, at least in a first approximation, the chains of kinds A, B, C and D may follow each other, according to a nearly random pattern. Further adjustments of the positions of the chains also leading to a slight increase of the average density should occur, in agreement with the experimental data, since the density is higher for the mesomorphic form than for form III of sPPMS. In brief, our model of the mesomorphic form of sPPMS is characterized by chains in a fixed all-*trans* conformation, with the axes placed, on average and in a first approximation, at the nodes of the orthorhombic lattice of form III of sPPMS. Still, as in the form III of sPPMS the phenyl groups alternate along a and b with the quote along z at 0 and $c/2$. At variance with the limit-ordered form III of sPPMS, the four kind of chains, A, B, C and D may instead follow each other according to a nearly random pattern along a and along b. Local correlations should exist, however, favouring the sequences present in form III of sPPMS as well as sequences of chains of kind BD and AC along the direction a.

We have calculated the square modulus of the structure factors (I) to be compared with the experimental diffraction data for disordered as well as for the limit-ordered model structure of form III. A good agreement with the experimental pattern was obtained for a disordered model structure where each lattice site may be occupied (with equal probability) by chains of kind A and D followed along

a by chains of kind B or C (still with equal probability). In this way the chains of kind A(B) are followed along a by chains of kind B(A) (as in the limit-ordered orthorhombic form III of sPPMS) or, with equal probability, by chains of kind C(D) (which is a situation highly favoured energetically). Terms accounting for the finite dimensions of the crystallites and for a paracrystalline disorder along a, b and c are included, multiplying the interference term between each couple of chains by terms of the kind[26]:

$$J = \exp\{-2\pi[(\mathbf{s}\cdot\mathbf{a})^2\sigma_a^2 + \zeta^2\sigma_c^2] + a/L_a\}^{n_a+1} \quad (1)$$

and

$$H = \exp\{-2\pi[(\mathbf{s}\cdot\mathbf{b})^2\sigma_b^2] + b/L_b\}^{n_b+1}$$

s is the scattering factor $2\sin\theta/\lambda$, L_a and L_b the average lengths of the crystallites along a and b, respectively; n_a and n_b are the number of chains placed between the couple of chains in question along the direction of the axes a and b, respectively; σ_a, σ_b and σ_c the standard deviations of the three axes, respectively. Translational disorder along z was introduced only between chains belonging to different b–c rows. Since the calculations were performed along the layer lines only, we did not account for the finite dimensions of the crystallites along c, because this is equivalent to multiply the calculated values of the diffraction intensity for a constant value, whatever the layer line. A thermal factor D was included as:

$$D = \exp(-B_\xi\xi^2/2)\exp(-B_\zeta\zeta^2/2) \quad (2)$$

In the following calculations: $\sigma_a = \sigma_b = 0.8$ Å and $\sigma_c = 1.0$ Å. The thermal factors B_ξ and B_ζ were fixed equal to 12 Å^2 and 6 Å^2, respectively, whereas $L_a = L_b = 30$ Å. The calculations for the ordered form III were also repeated for $L_a = L_b = 60$ Å. In order to better compare the calculated profiles with the experimental ones, for the smaller aggregates the background subtending the Bragg scattering (approximated through a hyperbola) was subtracted from the equatorial profiles.

RESULTS AND DISCUSSIONS

The calculated X-ray diffraction intensities (I) for the limit-ordered model structures of form III along the equator and the layer lines are reported in *Figure 6* for $L_a = L_b = 60$ Å (*Figure 6A*) and $L_a = L_b = 30$ Å (*Figure 6B*).

The main features of the diffraction pattern of the mesomorphic form of sPPMS are already present in the calculated profiles of *Figure 6*. In fact, they show the presence of a strong reflection on the first layer line centred at $\xi = 0.11$ Å^{-1}, a less intense peak on the third layer line centred at $\xi = 0.1$ Å^{-1}, and two meridional peaks on the second and the fourth layer lines, in qualitative agreement with the experimental patterns of *Figure 1B*. The calculated diffraction profile on the equator of *Figure 6A* is substantially different from the experimental one, however. In particular, in the pattern of the form III only three main peaks centred at $\xi \approx 0.08$ Å^{-1}, $\xi \approx 0.15$ Å^{-1} and at $\xi = 0.17$ Å^{-1} are apparent and the peak at $\xi \approx 0.12$ Å^{-1} is too weak with respect to the experimental case. The ratio between the integrated intensity of the peak on the first layer line and the integrated intensity along the equatorial profile in the range $0.06 < \xi < 0.25$ Å^{-1} ($I(1)/I(0)$) is nearly 1.5 in *Figure 6A* as well as in *Figure 6B*, not in agreement with the experimental value. The latter ratio is better approximated if some disorder is introduced in the small aggregate. The calculated X-ray diffraction profiles for the disordered model are plotted in *Figure 7*, as an example. Off the equator, the patterns of *Figure 7* present the same features as in *Figure 6B*. Moreover the equatorial pattern is now similar to the experimental one of *Figure 1B* and in particular a broad maximum centred at $\xi = 0.12$ Å^{-1} is apparent; also, the ratio $I(1)/I(0)$ increases to ≈ 4.4, as in the experimental case.

We did not hazard further calculations, because we believe that the mean structural features of the mesomorphic form of sPPMS are clarified in the present analysis. It consists of very small aggregates of chains in all-*trans* conformation, with axes placed on average and at least in first approximation, at the nodes of the orthorhombic lattice of the limit-ordered structural model of form III. The phenyl groups quoted at 0 and $\frac{1}{2}$ along c alternate along the axes a and b. The chains follow each other along the a and b directions according to a pattern that can be also different from that of the limit-ordered model of form III and local rearrangements of the chains, minimizing the packing energy, also slightly increasing the density of form III, should be allowed for. These disordered aggregates should be very small, consisting on average of not more than 4–5 rows of chains stacked along a and not more than 2–3 columns of chains stacked along b. The sequences AC and BD along a should be particularly favoured. The occurrence of these couples of chains, with the axes placed at an optimum distance (shorter than $a/2$), makes possible the juxtaposition of any other kind of chain after them (A, B, C, D) at a low cost of the packing energy, and gives rise to disorder.

CONCLUSIONS

An analysis of the structure of the mesomorphic form IV of sPPMS, through comparison between the experimental intensities, collected by an automatic diffractometer, and the calculated Fourier transforms of models, has been presented. The X-ray diffraction pattern of a fibre of sPPMS in the mesomorphic form is characterized by the absence of sharp reflections on the equator and by the presence of a strong peak on the first layer line and of two meridional peaks on the second and the fourth layer line, indicating a *trans*-planar conformation of the chains.

Packing energy as well as Fourier transform calculations have shown that all the models in which phenyl rings, quoted at 0 and $c/2$ along z, alternate along a and b are energetically feasible and show X-ray diffraction profiles in a qualitative agreement with the experimental ones. The ratio between the integrated intensities on the first layer line and on the equator can be accounted for by orthorhombic model structures of very small dimensions with a chain packing mode close to that one of the form III of sPPMS.

ACKNOWLEDGEMENTS

We wish to thank the Ministero dell' Università e della Ricerca Scientifica for financial support. X-ray diffraction data were recorded with a Nonius CAD4 automatic diffractometer (Centro Interdipartimentale di Metodologia Chimico-Fisica, University of Naples).

REFERENCES

1. Ishihara, N., Seimiya, T., Kuramoto, M. and Uoi, M., *Macromolecules*, 1986, **19**, 2465.
2. Zambelli, A., Longo, P., Pellecchia, C. and Grassi, A., *Macromolecules*, 1987, **20**, 2035.
3. Resconi, L., Albizzati, E., Giannini, U., Giunchi, G. and Mazzocchi, R., Italian Patent Application, 22827 A, 1986.
4. Ishihara, N., Kuramoto, M. and Uoi, M., European Patent Application, 0224097 A1, 1987.
5. Ishihara, N., Kuramoto, M. and Uoi, M., *Macromolecules*, 1988, **21**, 3356.
6. Pellecchia, C., Longo, P., Grassi, A., Ammendola, P. and Zambelli, A., *Makromol. Chem., Rapid Commun.*, 1987, **8**, 277.
7. Grassi, A., Pellecchia, C., Longo, P. and Zambelli, A., *Gazz. Chim. Ital.*, 1987, **20**, 2035.
8. Grassi, A., Longo, P., Proto, A. and Zambelli, A., *Macromolecules*, 1989, **22**, 104.
9. Immirzi, A., De Candia, F., Iannelli, P., Vittoria, V. and Zambelli, A., *Makromol. Chem., Rapid Commun.*, 1988, **9**, 761.
10. Guerra, G., Vitagliano, V. M., De Rosa, C., Petraccone, V. and Corradini, P., *Macromolecules*, 1990, **23**, 1539.
11. Chatani, Y., Shimane, Y., Inoue, Y., Inagaki, T., Ijitsu, T. and Yukinari, T., *Polymer*, 1992, **33**, 488.
12. De Rosa, C., Guerra, G., Petraccone, V. and Corradini, P., *Polymer J.*, 1991, **23**, 1435.
13. De Rosa, C., Rapacciuolo, M., Guerra, G., Petraccone, V. and Corradini, P., *Polymer*, 1992, **33**, 1423.
14. Petraccone, V., Auriemma, F., Dal Poggetto, F., De Rosa, C., Guerra, G. and Corradini, P., *Macromol. Chem.*, 1993, **194**, 1335; Auriemma, F., Petraccone, V., Dal Poggetto, F., De Rosa, C., Guerra, G., Manfredi, C. and Corradini, P., *Macromolecules*, 1993, **26**, 3772.
15. Corradini, P., De Rosa, C., Guerra, G., Napolitano, R., Petraccone, V. and Pirozzi, B., *Eur. Polym. J.*, 1994, **30**, 1173.
16. Chatani, Y., Shimane, Y., Ijitsu, T. and Yukinari, T., *Polymer*, 1993, **34**, 1625.
17. Chatani, Y., Shimane, Y., Inagaki, T., Ijitsu, T., Yukinari, T. and Shikuma, H., *Polymer*, 1993, **34**, 1620.
18. Chatani, Y., Inagaki, T., Shimane, Y. and Shikuma, H., *Polymer*, 1993, **34**, 4841.
19. Iuliano, M., Guerra, G., Petraccone, V., Corradini, P. and Pellecchia, C., *New Polymeric Material*, 1992, **3**, 133.
20. Guerra, G., Iuliano, M., Grassi, A., Rice, D. M., Karasz, F. E. and McKnight, W. J., *Polymer Commun.*, 1991, **32**, 430.
21. Guerra, G., Dal Poggetto, F., Iuliano, M. and Manfredi, C., *Makromol. Chem.*, 1992, **193**, 2413.
22. De Rosa, C., Petraccone, V., Guerra, G. and Manfredi, C., *Polymer*, 1996, **37**, 5247.
23. De Rosa, C., Petraccone, V., Dal Poggetto, F., Guerra, G., Pirozzi, B., Di Lorenzo, M. L. and Corradini, P., *Macromolecules*, 1995, **28**, 5507.
24. De Rosa, C., *Macromolecules*, 1996, **29**, 8460.
25. Greis, O., Xu, T., Asano, T. and Peterman, J., *Polymer*, 1989, **30**, 590.
26. Liu, X. D. and Ruland, W., *Macromolecules*, 1993, **26**, 3030.